

## Supplementary Information

### **Lessons learned from the comparison and combination of fine carbonaceous aerosol source apportionment at two locations in the city of Strasbourg, France**

Hasna Chebaicheb<sup>1,2,3</sup>, Mélodie Chatain<sup>4</sup>, Olivier Favez<sup>2,3</sup>, Joel F. de Brito<sup>1</sup>, Vincent Crenn<sup>5</sup>, Tanguy Amodeo<sup>2,3</sup>, Mohamed Gherras<sup>2</sup>, Emmanuel Jantzen<sup>4</sup>, Caroline Marchand<sup>2,3</sup>, Véronique Riffault<sup>1,3</sup>

<sup>1</sup>IMT Nord Europe, Institut Mines-Télécom, Université de Lille, Centre for Energy and Environment, 59000, Lille, France

<sup>2</sup>Institut National de l'environnement Industriel et des Risques (INERIS), 60550 Verneuil-en-Halatte, France

<sup>3</sup>Laboratoire Central de Surveillance de la Qualité de l'Air (LCSQA), 60550 Verneuil-en-Halatte, France

<sup>4</sup>Atmo Grand Est, 67300 Schiltigheim, France

<sup>5</sup>ADDAIR, F-78530 Buc, France

*Correspondence to:* hasna.chebaicheb@ineris.fr; melodie.chatain@atmo-grandest.eu

## S0. ACSM data analysis

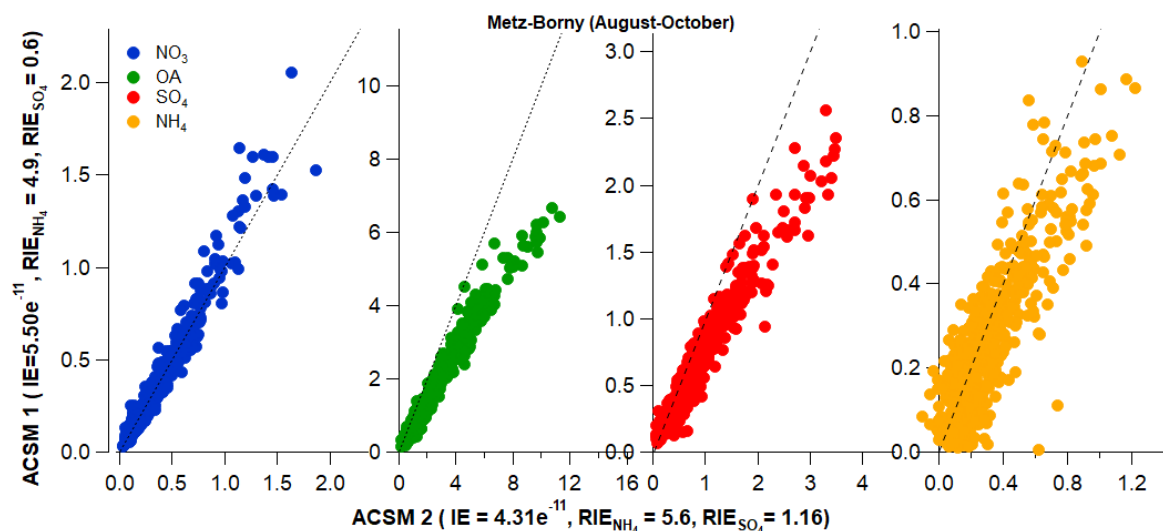


Figure S1: Scatter plots between ACSM #1 (further deployed at the Clemenceau site) and #2 (deployed at the Danube site) for non-refractory chemical species (OA,  $\text{NO}_3$ ,  $\text{NH}_4$ , and  $\text{SO}_4$ ), while measuring at the Metz-Borny site from August to October 2019. RIE refers to relative ionization efficiency.

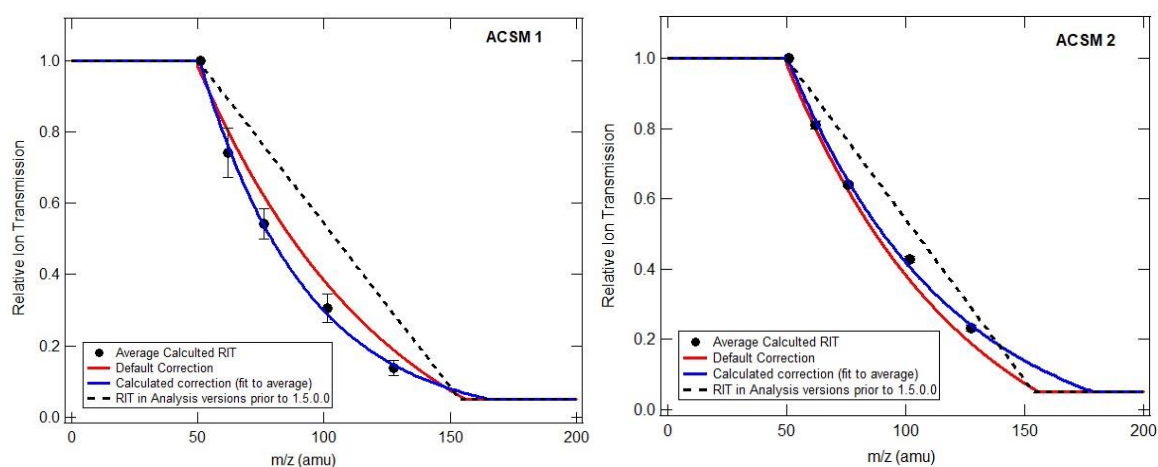


Figure S2: Relative ion transmission (RIT) as a function of  $m/z$  for ACSM #1 (Clemenceau) and #2 (Danube).

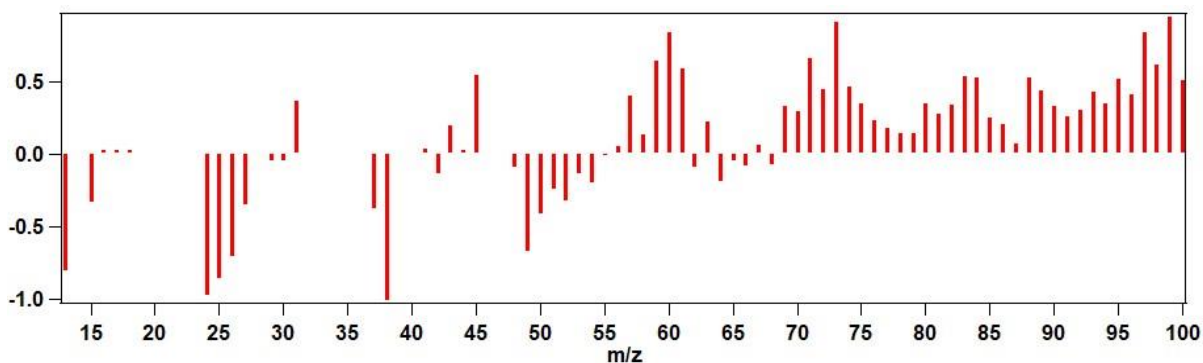
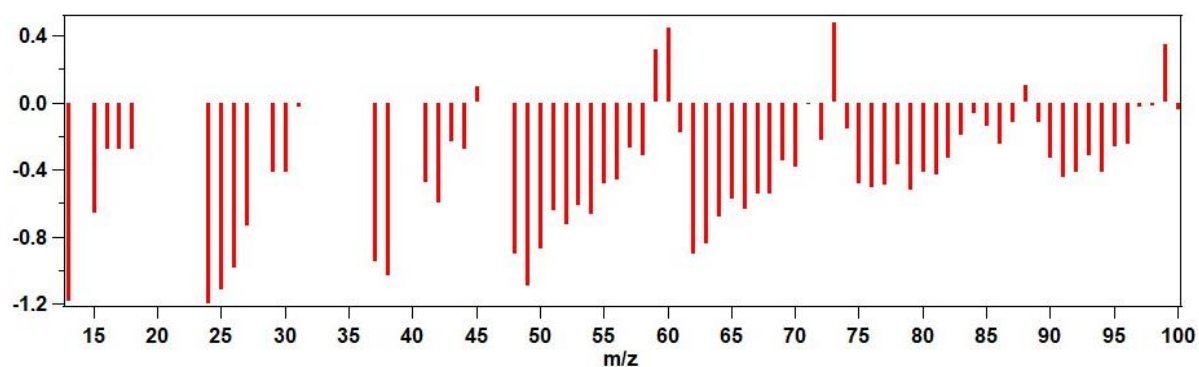


Figure S3: Comparison of the intensities of the different  $m/z$  fragments of the average OA mass spectra of ACSM #1 (Clemenceau) and #2 (Danube), normalized by the total OA intensity. Upper panel: during the pre-campaign intercomparison exercise in Metz-Borny; Lower panel: during concomitant measurements at both sites in Strasbourg.

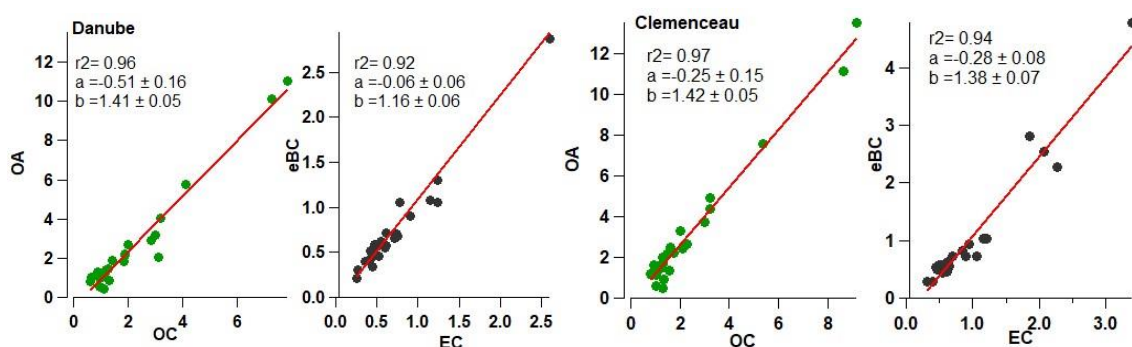
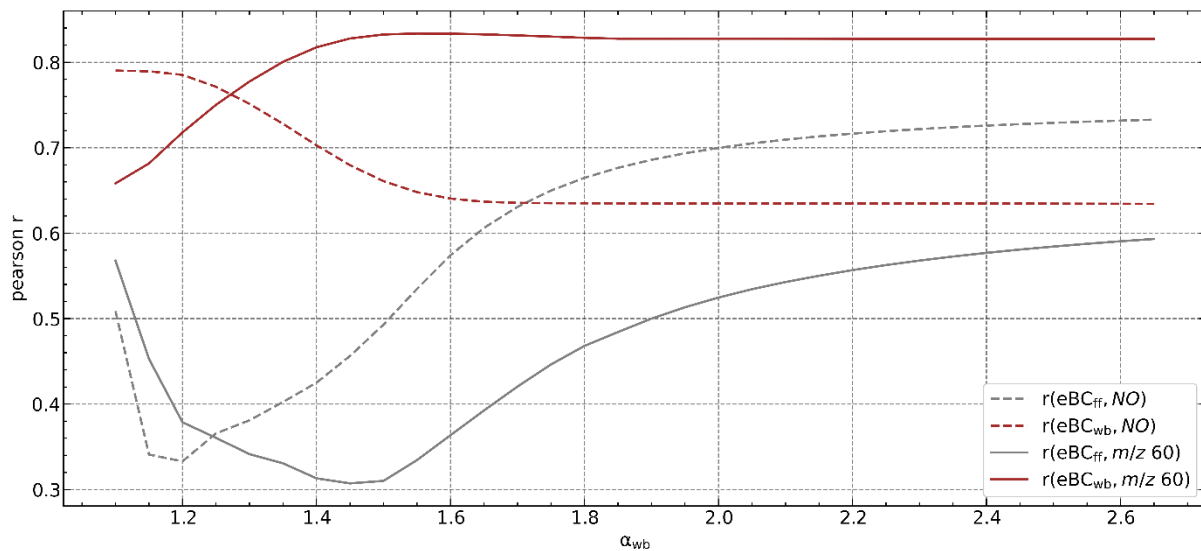
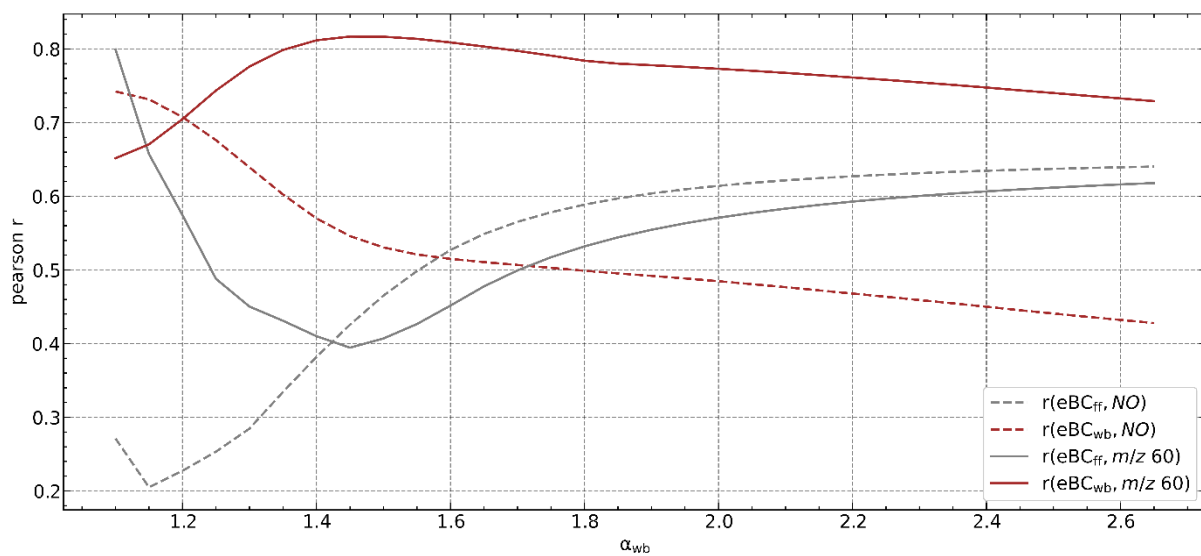


Figure S4: Scatter plots of OA vs. OC and eBC vs. EC in  $PM_1$  for both Strasbourg sites: Danube (left) and Clemenceau (right).

39



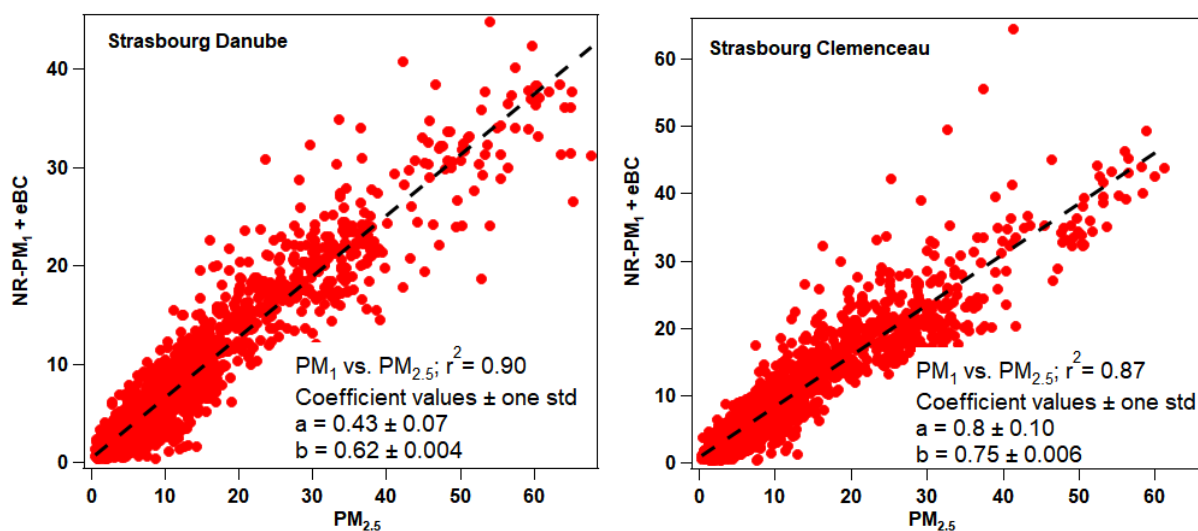
40



41

42 Figure S5: Determination of  $\alpha_{\text{ff}}$  and  $\alpha_{\text{wb}}$  values for the Danube (top) and Clemenceau (bottom) sites.

43



44

45 Figure S6: Comparison between Recalculated PM<sub>1</sub> (NR-PM<sub>1</sub> + eBC) and PM<sub>2.5</sub> for Strasbourg Danube (left) and  
 46 Strasbourg Clemenceau (right).

#### 47 S1. Individual PMF analysis

48 The 5-factor solution was chosen for the Clemenceau site. The two primary factors HOA and COA-like were  
 49 constrained using the reference profiles derived from Crippa et al. (2013) with a-values ranging from 0 to 0.3.  
 50 Multiple PMF tests were also carried out with a factor number ranging from 3 to 7. The 5-factor solution was  
 51 selected. Increasing the number of factors is not relevant, as it leads to OOA factors split. A specific factor 58-OA  
 52 was observed for solutions from 3 factors, highlighting the influence of this specific source. The 5 factors identified  
 53 were HOA, BBOA, COA-like, 58-OA, and OOA. Their identification was based on the study of their mass spectra  
 54 in comparison with reference profiles, their diel profiles, and correlations with external measurements.

55 The individual PMF applied for the Danube dataset was implemented in the same way as the Clemenceau site with  
 56 multiple PMF runs tested to identify the better solution (a-values between 0 to 0.3 for the HOA and COA-like  
 57 profiles, 3 to 7 number of factors). The presence of a COA-like was not relevant for this site, notably due to the  
 58 absence of a peak at midday. As the Danube site is more residential, there may not be as many people returning  
 59 for lunch, which could explain the only evening peak observed at this site. 5 factors were identified for this site as  
 60 well: HOA, BBOA, COA-like, 58-OA, and OOA.

61

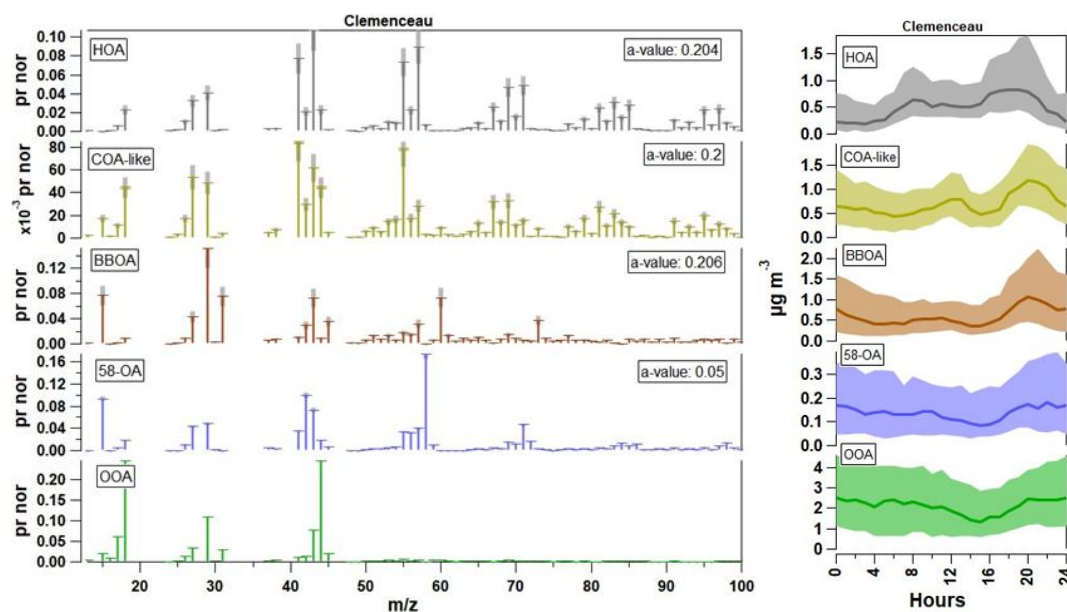


Figure S7: Mass spectra (left) and diel cycles (right) of OA factors for the Clemenceau site. The shaded areas represent the interquartile range and the bold line in the middle represents the median.

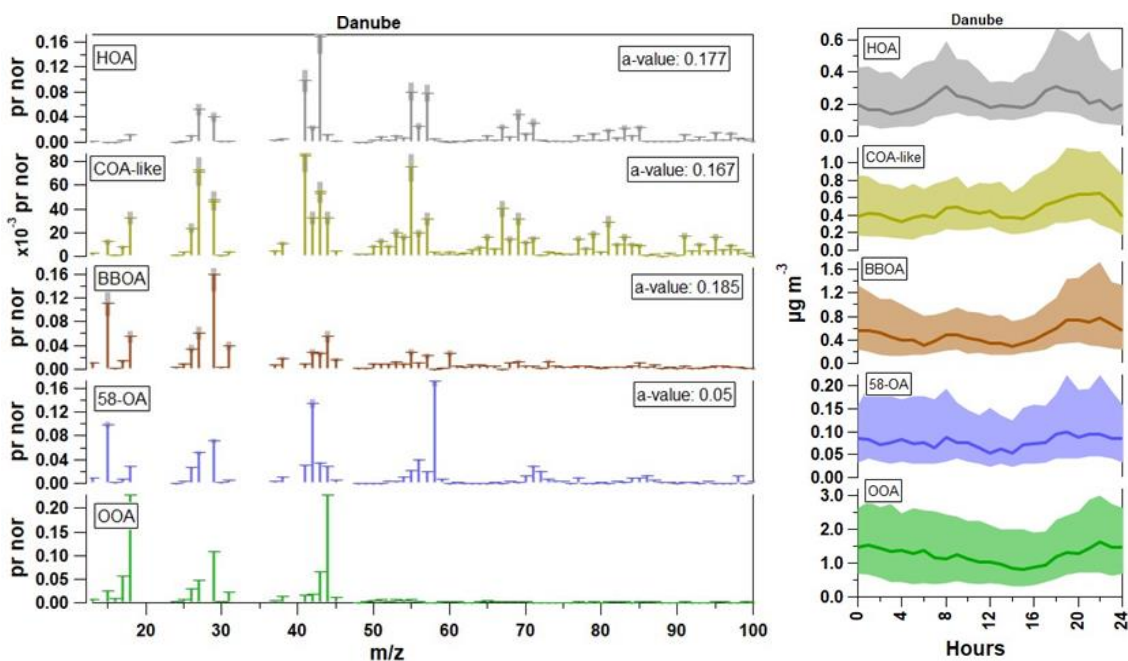


Figure S8: Mass spectra (left) and diel cycles (right) of OA factors for the Danube site. The shaded areas represent the interquartile range and the bold line in the middle represents the median.



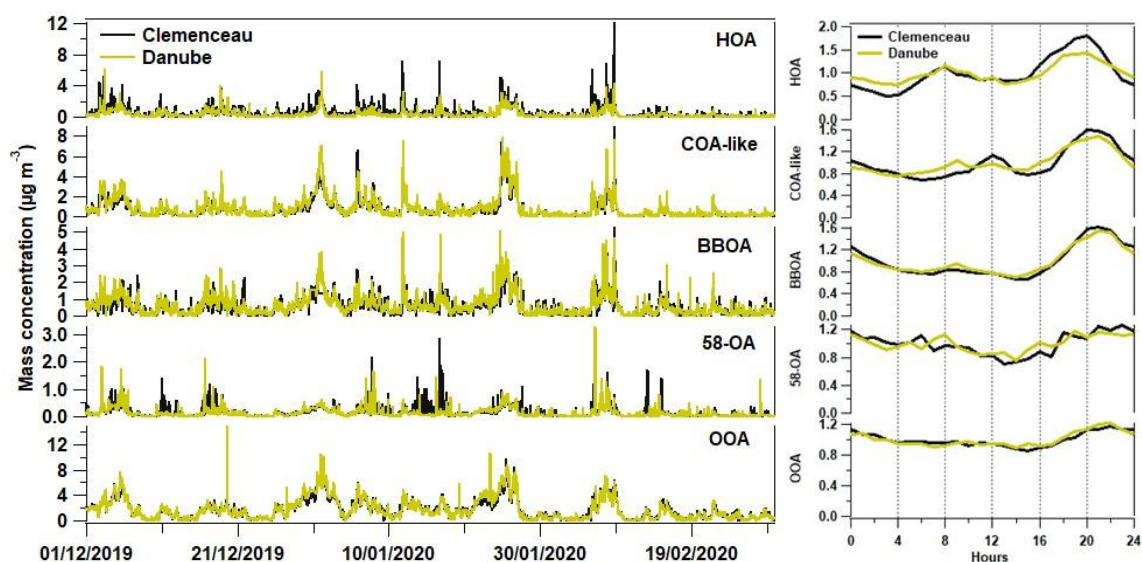


Figure S9: Time series (left) and normalized diel cycles (right) of OA factors from individual PMF at both sites during the studied period.

## S2. Combined PMF analysis

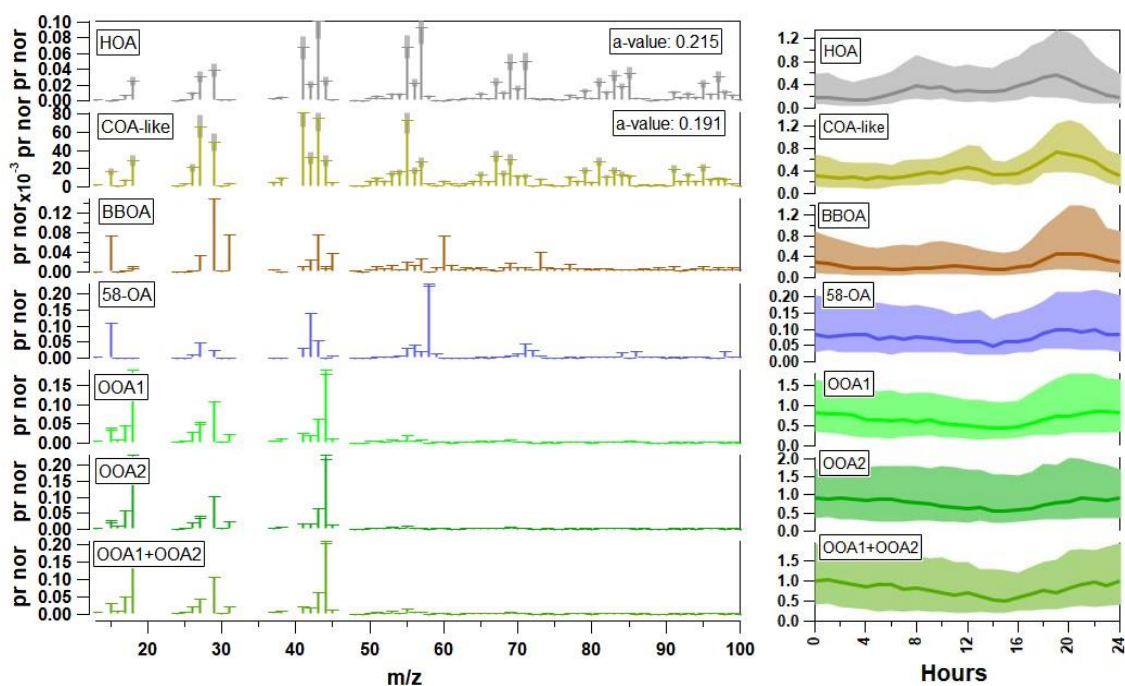


Figure S10: Mass spectra (left) and diel cycles (right) of OA factors for the combined PMF at both sites. The shaded areas represent the interquartile range and the bold line in the middle represents the median.

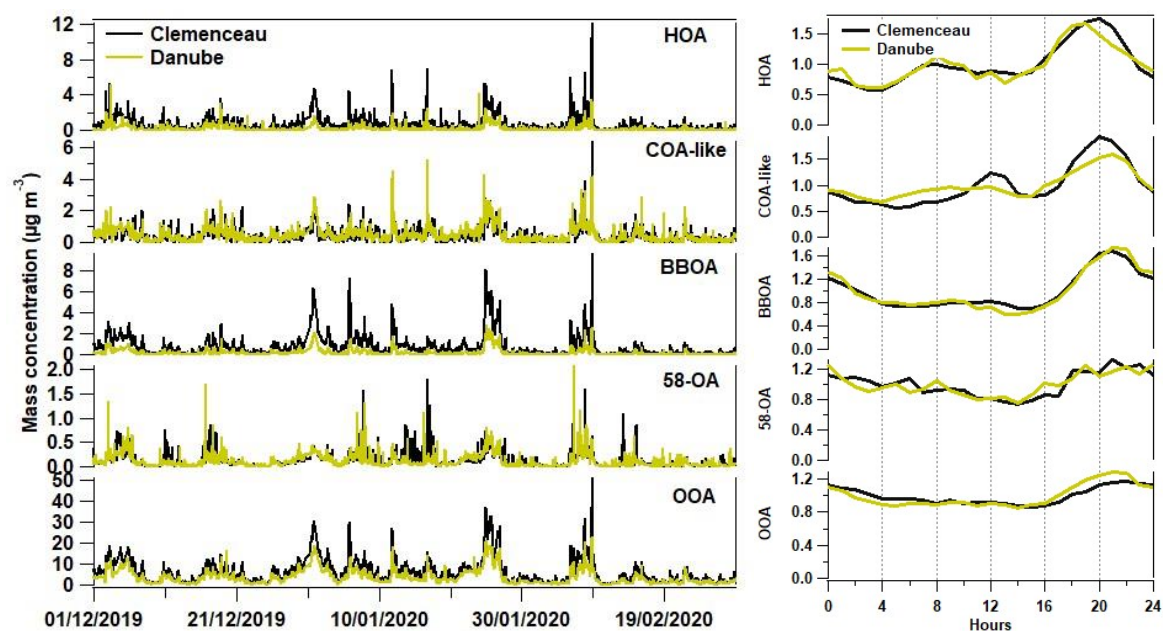


Figure S11: Time series (left) and normalized diel cycles (right) of OA factors from the combined PMF at both sites.

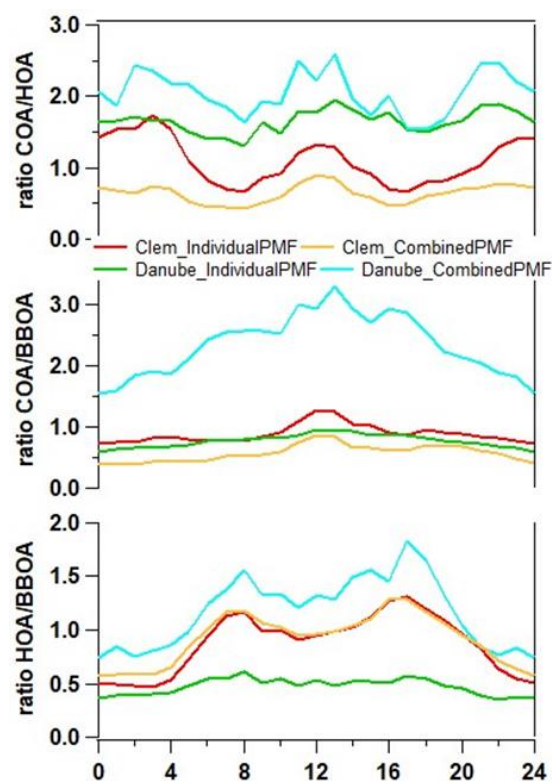


Figure S12: From top to bottom, diel cycles of the COA-like/HOA, COA-like/BBOA, and HOA/BBOA ratios for each PMF and site.



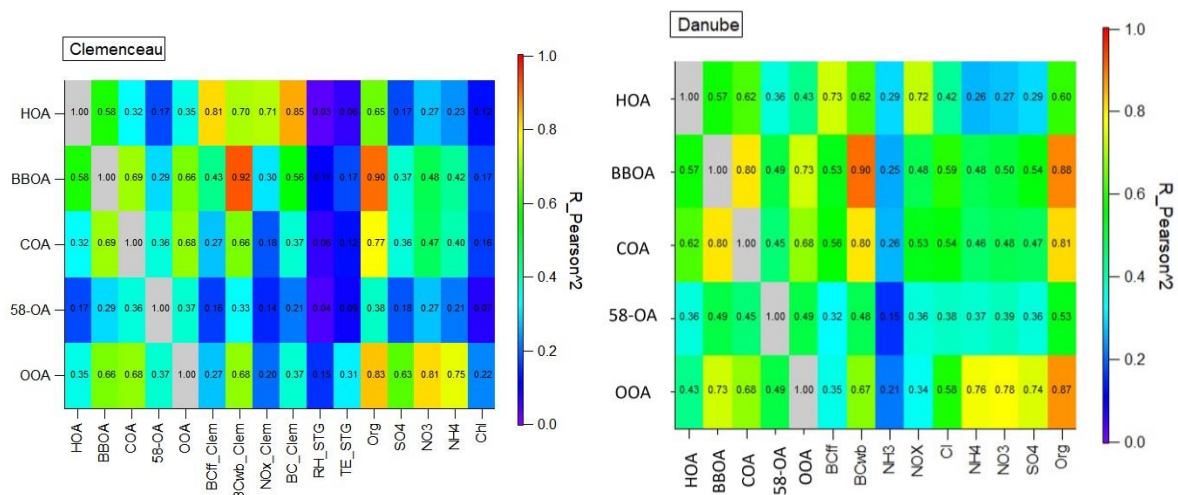


Figure S13: Correlations between OA factors and external variables for both sites

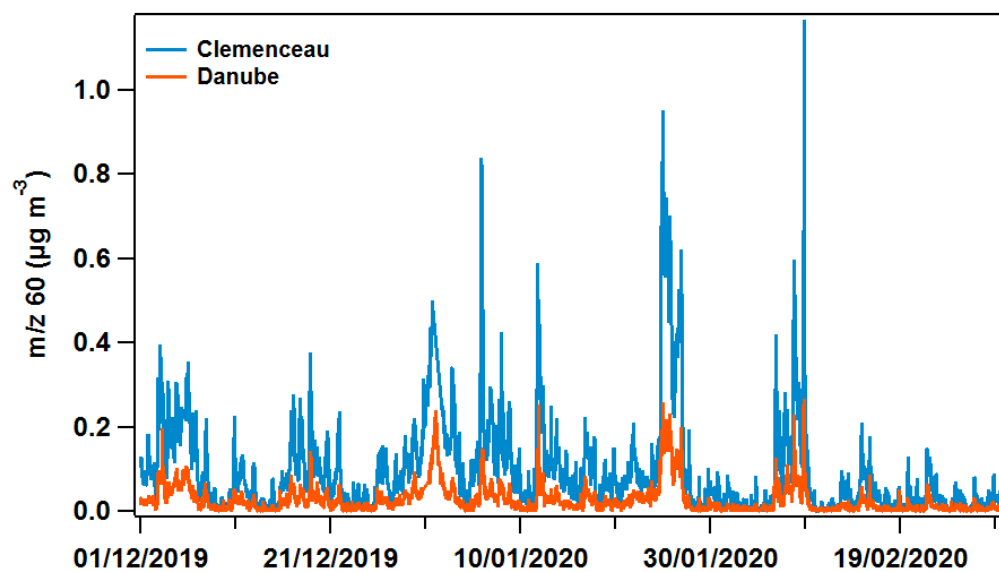


Figure S14: Time series of m/z 60 at the Danube and Clemenceau sites.

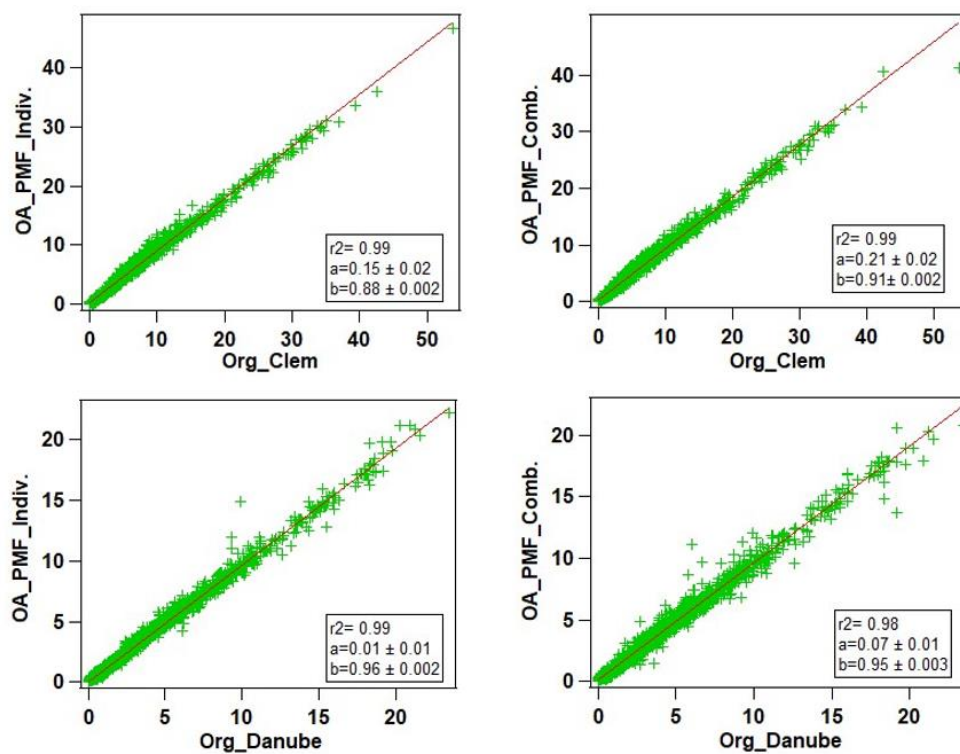


Figure S15: Scatterplots of OA (sum of the different OA factors) resolved in both PMFs vs. the organic mass concentration from ACSM at both sites.

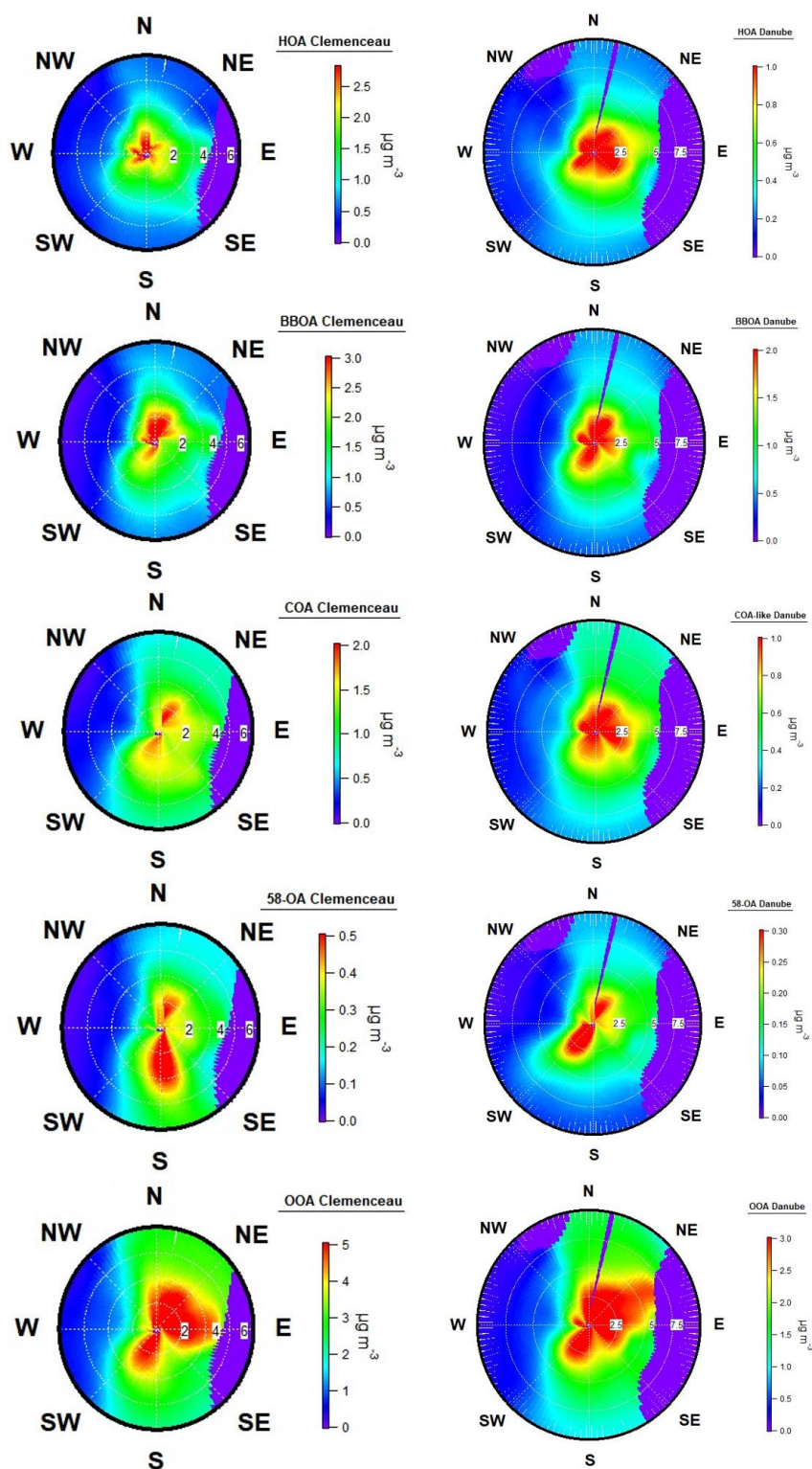


Figure S16: Pollution roses for OA factors, including HOA, BBOA, COA-like, 58-OA, and OOA at both sites: Clemenceau (left) and Danube (right).